Single Integral Equation for Electromagnetic Scattering by Three-Dimensional Homogeneous Dielectric Objects

Michael S. Yeung

Abstract— A single integral equation formulation for electromagnetic scattering by three-dimensional (3-D) homogeneous dielectric objects is developed. In this formulation, a single effective electric current on the surface S of a dielectric object is used to generate the scattered fields in the interior region. The equivalent electric and magnetic currents for the exterior region are obtained by enforcing the continuity of the tangential fields across S. A single integral equation for the effective electric current is obtained by enforcing the vanishing of the total field due to the exterior equivalent currents inside S. The single integral equation is solved by the method of moments. Numerical results for a dielectric sphere obtained with this method are in good agreement with the exact results. Furthermore, the convergence speed of the iterative solution of the matrix equation in this formulation is significantly greater than that of the coupled integral equations formulation.

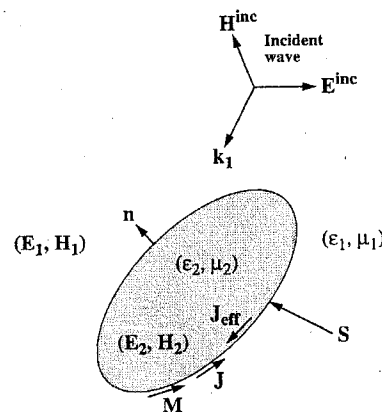*Index Terms*— Boundary integral equations, electromagnetic scattering, method of moments.

Fig. 1. Homogeneous dielectric object (ε_2, μ_2) embedded in a homogeneous medium (ε_1, μ_1). $(\mathbf{J}, \mathbf{M})$ are the equivalent currents for the exterior region. $\mathbf{J}_{\text{eff}}$ is a single effective electric current for the interior region.

I. INTRODUCTION

SURFACE integral equations are widely used to solve problems of electromagnetic scattering by an interface S between two homogeneous regions of space [1]. If one of the regions is a perfect electric conductor, it is sufficient to find the electric current on S by solving a single integral equation such as the electric field integral equation (EFIE), magnetic field integral equation (MFIE), or combined field integral equation (CFIE) [2]. In the case of dielectric media, the usual procedure is to solve a pair of coupled integral equations for the equivalent electric and magnetic currents on S [3]. Such a doubling in the number of unknowns may be undesirable due to increased computation time and storage requirement.

Maystre [4] first showed how a single unknown function on S can be employed to solve the problem of electromagnetic diffraction by a two-dimensional dielectric grating. Marx [5], [6] generalized Maystre's method to the scattering of an electromagnetic wave with arbitrary time dependence by a three-dimensional (3-D) dielectric object. Glisson [7] presented a single integral equation for 3-D dielectric objects in the frequency domain using the equivalence principle. However, no numerical results were given by Marx or Glisson.

In this paper, an alternative single integral equation for 3-D dielectric objects in the frequency domain is discussed. Furthermore, the single integral equation is solved by the method of moments and numerical results are presented.

The formulation of the single integral equation is discussed in Section II. The expansion of the surface current densities in triangular-patch basis functions is discussed in Section III. The solution of the single integral equation by the method of moments is discussed in Section IV and numerical results for a dielectric sphere are presented in Section V. The problem of internal resonance is discussed in Appendix B.

II. SINGLE INTEGRAL EQUATION FORMULATION

Referring to Fig. 1, let S denote the surface of a 3-D homogeneous dielectric object illuminated by an incident plane wave. The regions exterior and interior to the object are characterized by material parameters (μ_1, ε_1) and (μ_2, ε_2), respectively. The total fields $(\mathbf{E}_1, \mathbf{H}_1)$ in the exterior region are given by the sums of the incident fields $(\mathbf{E}^{\text{inc}}, \mathbf{H}^{\text{inc}})$ and the fields radiated by a set of equivalent currents $(\mathbf{J}, \mathbf{M})$ on S

$$\mathbf{E}_1 = \mathbf{E}^{\text{inc}} + \hat{\mathbf{E}}_1^s(\mathbf{J}, \mathbf{M})\big|_{\text{outside } S} \tag{1}$$

$$\mathbf{H}_1 = \mathbf{H}^{\text{inc}} + \hat{\mathbf{H}}_1^s(\mathbf{J}, \mathbf{M})\big|_{\text{outside } S} \tag{2}$$

where $\hat{\mathbf{E}}_1^s$ and $\hat{\mathbf{H}}_1^s$ are integral operators for the exterior region. The explicit forms of these integral operators are given in Appendix A. By the equivalence principle, the equivalent

currents are related to the total tangential fields on S by

$$J = n \times H_1 \big|_{\text{just outside } S} \tag{3}$$

$$M = -n \times E_1 \big|_{\text{just outside } S}. \tag{4}$$

where n is the unit normal to S pointing out of the object.

Taking into account the discontinuous behavior of the integral operators $\hat{E}_1^s$ and $\hat{H}_1^s$ across S (the jump condition), (3) and (4) imply that the quantities defined by (1) and (2) vanish everywhere inside the object

$$E^{\text{inc}} + \hat{E}_1^s(J, M) \big|_{\text{inside } S} = 0 \tag{5}$$

$$H^{\text{inc}} + \hat{H}_1^s(J, M) \big|_{\text{inside } S} = 0. \tag{6}$$

In the usual coupled integral equations method [3], the fields (E_2, H_2) in the interior region are expressed in terms of the same pair of equivalent currents (J, M), but with the opposite sign by

$$E_2 = \hat{E}_2^s(-J, -M) \big|_{\text{inside } S} \tag{7}$$

$$H_2 = \hat{H}_2^s(-J, -M) \big|_{\text{inside } S} \tag{8}$$

where $\hat{E}_2^s$ and $\hat{H}_2^s$ are integral operators for the interior region. Alternatively, the fields in the interior region can be represented by a single effective electric current J_{eff}

$$E_2 = \hat{E}_2^s(J_{\text{eff}}, 0) \big|_{\text{inside } S} \tag{9}$$

$$H_2 = \hat{H}_2^s(J_{\text{eff}}, 0) \big|_{\text{inside } S} \tag{10}$$

or by a single effective magnetic current M_{eff}

$$E_2 = \hat{E}_2^s(0, M_{\text{eff}}) \big|_{\text{inside } S} \tag{11}$$

$$H_2 = \hat{H}_2^s(0, M_{\text{eff}}) \big|_{\text{inside } S}. \tag{12}$$

It should be noted that the effective current J_{eff} or M_{eff} radiates the correct fields only in the interior region. That the representation (9) and (10) or the representation (11) and (12) is plausible is suggested by the fact that the fields (E_2, H_2) given by (9) and (10) or by (11) and (12) certainly satisfy Maxwell's equations for the interior region for arbitrary J_{eff} or M_{eff}. It remains to show that the necessary boundary conditions can also be made to be satisfied.

In this paper, the representation in terms of the effective electric current J_{eff} is used. By evaluating the right-hand sides (RHS) of (9) and (10) at a point just inside S, the tangential fields just inside S can be found. Then, by enforcing the continuity of the tangential fields across S, the equivalent currents (J, M) for the exterior region are obtained

$$J = n \times \hat{H}_2^s(J_{\text{eff}}, 0) \big|_{\text{just inside } S} \tag{13}$$

$$M = -n \times \hat{E}_2^s(J_{\text{eff}}, 0) \big|_{\text{just inside } S}. \tag{14}$$

A single integral equation for J_{eff} is obtained by substituting (13) and (14) into either the EFIE (5) or the MFIE (6). For the EFIE, one obtains

$$-E^{\text{inc}} = \hat{E}_1^s\big[n \times \hat{H}_2^s(J_{\text{eff}}, 0), -n \times \hat{E}_2^s(J_{\text{eff}}, 0)\big] \big|_{\text{inside } S} \tag{15}$$
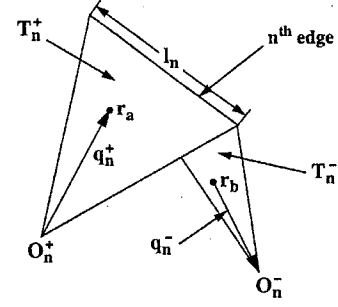

Fig. 2. Triangle pair (T_n^+, T_n^-) associated with the nth edge. Points r_a and r_b in (T_n^+, T_n^-) are measured by the vectors q_n^+ and q_n^- defined with respect to the vertices O_n^+ and O_n^-, respectively.

while for the MFIE, one obtains

$$-H^{\text{inc}} = \hat{H}_1^s\big[n \times \hat{H}_2^s(J_{\text{eff}}, 0), -n \times \hat{E}_2^s(J_{\text{eff}}, 0)\big] \big|_{\text{inside } S}. \tag{16}$$

In the above two equations, the integral operators $\hat{H}_2^s$ and $\hat{E}_2^s$ are evaluated at points just inside the object.

Once the effective current J_{eff} has been found by solving the single integral equation (15) or (16), the fields in the interior region are found from (9) and (10). The equivalent currents (J, M) for the exterior region are found from (13) and (14). The fields in the exterior region are then found from (1) and (2). In the absence of internal resonance, the fields so obtained are the correct fields because: 1) the fields in the interior region satisfy Maxwell's equations for this region [by (9) and (10)]; 2) the tangential fields are continuous across S [by (13) and (14)]; and 3) the fields in the exterior region satisfy Maxwell's equations for this region and the boundary condition at infinity [by (1) and (2)]. In the presence of internal resonance, however, condition 2) may not hold. This problem is discussed in Appendix B.

III. CURRENT BASIS FUNCTIONS

In order to transform the single integral equation (15) or (16) into a matrix equation, the surface S is replaced by a triangular-patch model and the unknown effective current J_{eff} is expanded in vector basis functions associated with the edges of the triangulated surface [8]. Fig. 2 shows two triangles T_n^+ and T_n^- associated with an edge n of the triangular-patch model of S. Points in T_n^+ are defined by the position vector q_n^+ pointing from the vertex O_n^+ of T_n^+ opposite the edge n. Similarly, points in T_n^- are defined by the position vector q_n^- pointing toward the vertex O_n^- of T_n^- opposite the edge n. A vector basis function f_n is associated with the edge n

$$f_n(r) = \begin{cases} \frac{l_n}{2A_n^+} q_n^+, & r \text{ in } T_n^+ \\ \frac{l_n}{2A_n^-} q_n^-, & r \text{ in } T_n^- \\ 0, & \text{otherwise} \end{cases} \tag{17}$$

where l_n is the length of the common edge n and $A_n^{\pm}$ are the areas of the triangles $T_n^{\pm}$.

The effective current $\mathbf{J}_{\text{eff}}$ is expanded in the vector basis functions $\mathbf{f}_n$

$$\mathbf{J}_{\text{eff}}(\mathbf{r}) = \sum_{n=1}^{N} \xi_n \mathbf{f}_n(\mathbf{r}) \qquad (18)$$

where N is the total number of edges in the triangular-patch model of S and ξ_n are the unknown current coefficients.

If the effective current (18) were substituted directly into the single integral equation (15) or (16), the RHS of the resulting equation would be difficult to evaluate because of integrations over the singularities in the integral operators $\hat{\mathbf{E}}_1^s$, $\hat{\mathbf{H}}_1^s$, $\hat{\mathbf{H}}_2^s$, and $\hat{\mathbf{E}}_2^s$. Instead, it is more convenient to expand the arguments of the integral operator $\hat{\mathbf{E}}_1^s$ or $\hat{\mathbf{H}}_1^s$, which are the tangential fields $\mathbf{n} \times \mathbf{H}_2$ and $-\mathbf{n} \times \mathbf{E}_2$ just inside S in the vector basis functions $\mathbf{f}_n$. Thus, one writes

$$\mathbf{n} \times \mathbf{H}_2(\mathbf{r}_-) = \sum_{i=1}^{N} I_i^e \mathbf{f}_i(\mathbf{r}) \qquad (19)$$

$$-\mathbf{n} \times \mathbf{E}_2(\mathbf{r}_-) = \sum_{i=1}^{N} I_i^m \mathbf{f}_i(\mathbf{r}) \qquad (20)$$

where $\mathbf{E}_2$ and $\mathbf{H}_2$ are given by (9) and (10), respectively, for a point $\mathbf{r}_-$ which approaches the point $\mathbf{r}$ on S from the interior region and (I_i^e, I_i^m) are the expansion coefficients to be determined.

Let $\mathbf{r}$ be a point on triangle T_n^+ which approaches the edge n and $\mathbf{l}_n$ be a unit vector lying along this edge. Also, let $\mathbf{n}$ be the unit normal to T_n^+ pointing out of the object. Using simple vector identities, one obtains

$$\mathbf{H}_2(\mathbf{r}_-) \cdot \mathbf{l}_n = -\mathbf{n} \cdot \{[\mathbf{n} \times \mathbf{H}_2(\mathbf{r}_-)] \times \mathbf{l}_n\}$$

$$= -\mathbf{n} \cdot \left\{ \sum_{i=1}^{N} I_i^e \mathbf{f}_i(\mathbf{r}) \times \mathbf{l}_n \right\}$$

$$= \sum_{i=1}^{N} I_i^e (\mathbf{n} \times \mathbf{l}_n) \cdot \mathbf{f}_i(\mathbf{r}) \qquad (21)$$

where (19) has been employed and use has been made of the fact that $\mathbf{n} \cdot \mathbf{l}_n = 0$.

The quantity $(\mathbf{n} \times \mathbf{l}_n) \cdot \mathbf{f}_i(\mathbf{r})$ in (21) is the component of the vector basis function $\mathbf{f}_i$ normal to the common edge n of the triangles $T_n^{\pm}$. Since the point $\mathbf{r}$ is infinitesimally close to the edge n, this quantity is nonzero only for $i = n$, as can be seen by examining the definition (17) of the vector basis function. Hence, (21) reduces to

$$\mathbf{H}_2(\mathbf{r}_-) \cdot \mathbf{l}_n = I_n^e (\mathbf{n} \times \mathbf{l}_n) \cdot \mathbf{f}_n(\mathbf{r}). \qquad (22)$$

It is well-known that the RHS of (22), which is the component of the vector basis function $\mathbf{f}_n$ normal to its defining edge n, is continuous across the edge n [8]. Hence, the RHS of (22) has a unique limit whether $\mathbf{r}$ approaches the edge n from T_n^+ or from T_n^-. Furthermore, this limit is independent of position along the edge n. Hence, the RHS of (22) is constant along the edge n, while the left-hand side of this equation in general varies along the edge n. This inconsistency is due to the fact that the expansion (19) is only an approximate representation of the vector field $\mathbf{n} \times \mathbf{H}_2$ on the surface S. However, one can

require (22) to be satisfied in an average sense by integrating both sides of this equation along the common edge n. This way, the expansion coefficients I_n^e for the equivalent electric current are found to be

$$I_n^e = -\frac{1}{l_n} \int_{l_n} dl \, \mathbf{H}_2(\mathbf{r}_-) \cdot \mathbf{l}_n. \qquad (23)$$

Similarly, the expansion coefficients I_n^m for the equivalent magnetic current are given by

$$I_n^m = \frac{1}{l_n} \int_{l_n} dl \, \mathbf{E}_2(\mathbf{r}_-) \cdot \mathbf{l}_n. \qquad (24)$$

In (23) and (24), the direction of the unit vector $\mathbf{l}_n$ has been chosen in such a way that if a right-hand screw through the triangle T_n^+ were rotated in the sense of the vector $\mathbf{l}_n$, it would advance in the direction of the unit normal $\mathbf{n}$ to T_n^+.

IV. SOLUTION BY THE METHOD OF MOMENTS

In the method of moments, the integral equation to be solved is tested with respect to suitable testing functions. For the EFIE (15), the usual testing procedure is to take the dot product of both sides of this equation with each vector basis function $\mathbf{f}_n$ and integrate the result over the domain of support of $\mathbf{f}_n$ [8]. For the MFIE (16), an alternative testing procedure is to take the dot product of both sides of this equation with the unit vector $\mathbf{l}_n$ lying along each edge n and integrate the result along the edge n [9].

To construct the moment-method matrix, the coefficients I_i^e and I_i^m are first computed from the coefficients ξ_j

$$\begin{bmatrix} I^e \\ I^m \end{bmatrix} = \begin{bmatrix} W^e \\ W^m \end{bmatrix} [\xi] \qquad (25)$$

where I^e, I^m and ξ are length-N column vectors of the respective coefficients and W^e and W^m are $N \times N$ matrices. The elements of these matrices are obtained by using (9), (10), (18) (23), and (24), and the known forms of the integral operators $\hat{\mathbf{E}}_2^s$ and $\hat{\mathbf{H}}_2^s$ given in Appendix A

$$W_{ij}^e = -\frac{\alpha_i}{2\pi} \delta_{ij} + \frac{1}{l_i} P \int_{l_i} dl \int_{T_j} dS' \, \mathbf{l}_i \cdot \mathbf{f}_j(\mathbf{r}') \times \nabla G_2(\mathbf{r} - \mathbf{r}') \qquad (26)$$

$$W_{ij}^m = -\frac{j\omega\mu_2}{l_i} \int_{l_i} dl \int_{T_j} dS' \, \mathbf{l}_i \cdot \mathbf{f}_j(\mathbf{r}') G_2(\mathbf{r} - \mathbf{r}')$$

$$- \frac{j}{\omega\varepsilon_2 l_i} \int_{T_j} dS' \, \nabla' \cdot \mathbf{f}_j(\mathbf{r}') [G_2(\mathbf{r}_i^{(+)} - \mathbf{r}')$$

$$- G_2(\mathbf{r}_i^{(-)} - \mathbf{r}')]. \qquad (27)$$

In the above equations, α_i is the angle between the planes of the triangles T_i^+ and T_i^- measured in the exterior region, $T_j = T_j^+ + T_j^-$ and P means that the term with $i = j$ is to be omitted. Also, $\mathbf{r}_i^{(+)}$ and $\mathbf{r}_i^{(-)}$ are the two endpoints of the edge i, such that the unit vector $\mathbf{l}_i$ points from $\mathbf{r}_i^{(-)}$ to $\mathbf{r}_i^{(+)}$ and $G_2(\mathbf{r} - \mathbf{r}')$ is the Green's function for the interior region

$$G_2(\mathbf{r} - \mathbf{r}') = \frac{e^{-jk_2|\mathbf{r} - \mathbf{r}'|}}{4\pi|\mathbf{r} - \mathbf{r}'|} \qquad (28)$$

k_2 being the wavevector in the interior region.

Next, the moment-method matrix equation is constructed from the current coefficients I_n^e and I_n^m

$$[U^e \quad U^m]\begin{bmatrix} I^e \\ I^m \end{bmatrix} = [b] \qquad (29)$$

where U^e and U^m are $N \times N$ matrices and b is a length-N column vector of the incident excitation. For the EFIE (15), one takes the dot product of both sides of this equation with each vector basis function $\mathbf{f}_i$ and integrates the result over the corresponding triangle pair $T_i = T_i^+ + T_i^-$. Using (19) and (20) and the known form of the integral operator $\hat{\mathbf{E}}_1^s$ given in Appendix A, the elements of the matrices $U^{e(\text{EFIE})}$ and $U^{m(\text{EFIE})}$ for the EFIE are obtained

$$U_{ij}^{e(\text{EFIE})} = -j\omega\mu_1 \int_{T_i} dS \int_{T_j} dS' \, \mathbf{f}_i(\mathbf{r})\mathbf{f}_j(\mathbf{r}')$$
$$\times G_1(\mathbf{r} - \mathbf{r}') + \frac{j}{\omega\varepsilon_1} \int_{T_i} dS \int_{T_j} dS'$$
$$\times \nabla\mathbf{f}_i(\mathbf{r})\nabla' \cdot \mathbf{f}_j(\mathbf{r}')G_1(\mathbf{r} - \mathbf{r}') \qquad (30)$$

$$U_{ij}^{m(\text{EFIE})} = \int_{T_i} dS \int_{T_j} dS' [\mathbf{f}_i(\mathbf{r}) \times \mathbf{f}_j(\mathbf{r}')] \cdot \nabla G_1(\mathbf{r} - \mathbf{r}') \qquad (31)$$

and the excitation vector is given by

$$b_i^{(\text{EFIE})} = -\int_{T_i} dS \, \mathbf{E}^{\text{inc}}(\mathbf{r}) \cdot \mathbf{f}_i(\mathbf{r}). \qquad (32)$$

In (30) and (31), $G_1(\mathbf{r} - \mathbf{r}')$ is the Green's function for the exterior region

$$G_1(\mathbf{r} - \mathbf{r}') = \frac{e^{-jk_1|\mathbf{r} - \mathbf{r}'|}}{4\pi|\mathbf{r} - \mathbf{r}'|} \qquad (33)$$

k_1 being the wavevector in the exterior region.

For the MFIE (16), one takes the dot product of both sides of this equation with the unit vector $\mathbf{l}_i$ along each edge i and integrates the result along the edge i. Using (19) and (20) and the known form of the integral operator $\hat{\mathbf{H}}_1^s$ given in Appendix A, the elements of the matrices $U^{e(\text{MFIE})}$ and $U^{m(\text{MFIE})}$ for the MFIE are obtained

$$U_{ij}^{e(\text{MFIE})} = \frac{\alpha_i l_i}{2\pi}\delta_{ij} - P\int_{l_i} dl \int_{T_j} dS' \, \mathbf{l}_i \cdot \mathbf{f}_j(\mathbf{r}')$$
$$\times \nabla G_1(\mathbf{r} - \mathbf{r}') \qquad (34)$$

$$U_{ij}^{m(\text{MFIE})} = -j\omega\varepsilon_1 \int_{l_i} dl \int_{T_j} dS' \, \mathbf{l}_i \cdot \mathbf{f}_j(\mathbf{r}')G_1(\mathbf{r} - \mathbf{r}')$$
$$- \frac{j}{\omega\mu_1} \int_{T_j} dS' \, \nabla' \cdot \mathbf{f}_j(\mathbf{r}')[G_1(\mathbf{r}_i^{(+)} - \mathbf{r}')$$
$$- G_1(\mathbf{r}_i^{(-)} - \mathbf{r}')] \qquad (35)$$

and the excitation vector is given by

$$b_i^{(\text{MFIE})} = -\int_{l_i} dl \, \mathbf{H}^{\text{inc}}(\mathbf{r}) \cdot \mathbf{l}_i. \qquad (36)$$

Combining (29) and (25), the moment-method matrix equation for the unknown coefficients ξ_n can be written as
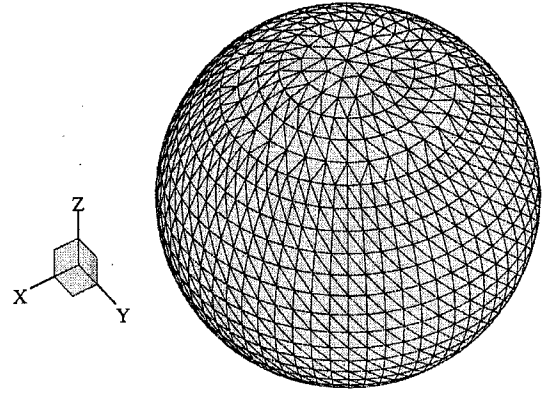
$$[Z][\xi] = [b] \qquad (37)$$

Fig. 3. Triangular-patch model of a dielectric sphere with $k_1 a = 1.0$. The number of triangles is 2400 and the number of edges is 3600. The sphere is illuminated by a plane wave traveling in the $+z$ direction and polarized with the electric vector in the x direction.

where Z is an $N \times N$ matrix constructed from the product of an $N \times 2N$ and a $2N \times N$ matrix

$$[Z] = [U^e \quad U^m]\begin{bmatrix} W^e \\ W^m \end{bmatrix}. \qquad (38)$$

The above discussion has been based on the representation (9) and (10) of the fields in the *interior* region in terms of an effective electric current $\mathbf{J}_{\text{eff}}$. Alternatively, one can start with a representation of the scattered fields in the *exterior* region in terms of an effective electric current as was done in [7]. From a programming point of view, the two approaches are similar in complexity since the present approach requires the application of the integral operators $\hat{\mathbf{E}}_2^s$ and $\hat{\mathbf{H}}_2^s$ to the *computed* effective current $\mathbf{J}_{\text{eff}}$, in accordance with (13) and (14), in order to find the scattered field in the exterior region, whereas the approach of [7] requires the application of the operator $\hat{\mathbf{E}}_2^s$ to the *incident* equivalent currents $(\mathbf{n} \times \mathbf{H}^{\text{inc}}, -\mathbf{n} \times \mathbf{E}^{\text{inc}})$ before the single integral equation is solved, in order to set up the corresponding excitation vector. However, numerical experiments have indicated that the present approach based on the representation (9) and (10) generally leads to greater convergence speed of the iterative solution, especially for dielectric objects with large dielectric constants.

Other formulations based on the representation of the interior or exterior scattered fields in terms of a single effective *magnetic* current $\mathbf{M}_{\text{eff}}$ are also possible. However, numerical experiments have indicated that such an approach generally leads to lower convergence speed of the iterative solution than the approach discussed in this paper.

V. NUMERICAL RESULTS

The single integral equations discussed in the last section were tested on the problem of electromagnetic scattering of a plane wave by a dielectric sphere. The surface of the sphere was modeled by triangular patches with an average side length Δ in the range $\lambda_2/25 < \Delta < \lambda_2/12$, where λ_2 is the wavelength inside the sphere. To reduce computation time, the matrix equation (37) was solved iteratively by the generalized minimum residual (GMRES) method [10].

The triangular-patch model for a sphere with $k_1 a = 1.0$ and $N = 3600$ is shown in Fig. 3, where a is the radius of the sphere and N is the total number of edges. The
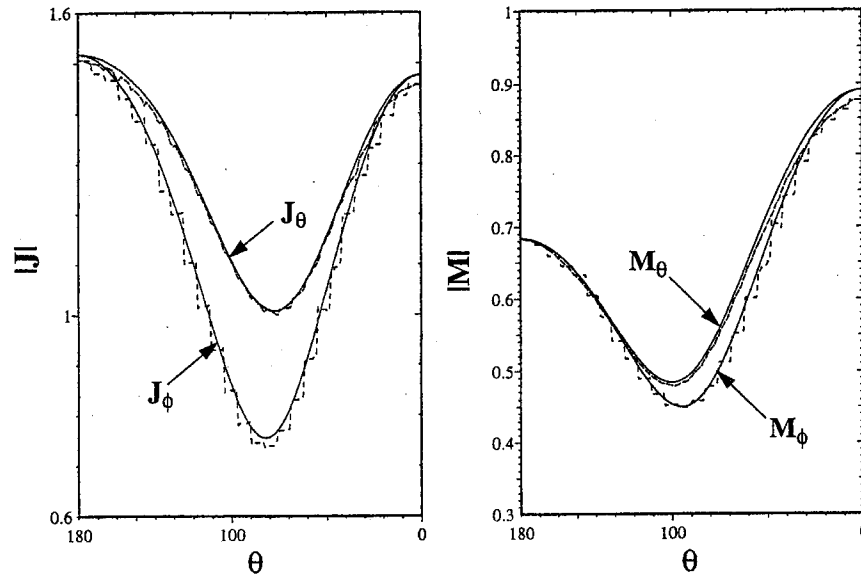
Fig. 4. Equivalent electric ($\mathbf{J}$) and magnetic ($\mathbf{M}$) currents induced on a dielectric sphere with $\varepsilon_2 = 4.0$ and $k_1 a = 1.0$. Solid lines are the exact results. Dashed lines are the results of the single integral equation method.
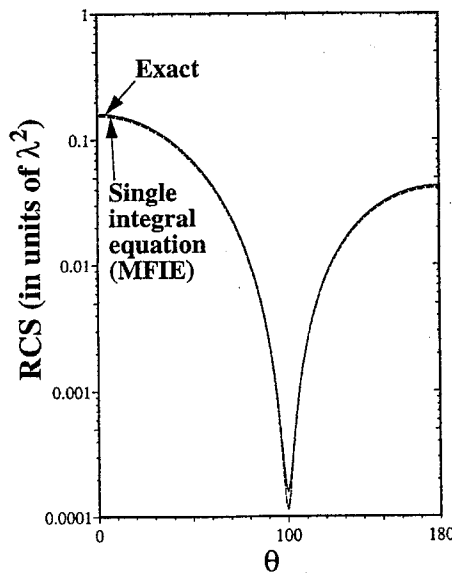

Fig. 5. Radar cross section of a dielectric sphere with $\varepsilon_2 = 4.0$ and $k_1 a = 1.0$.
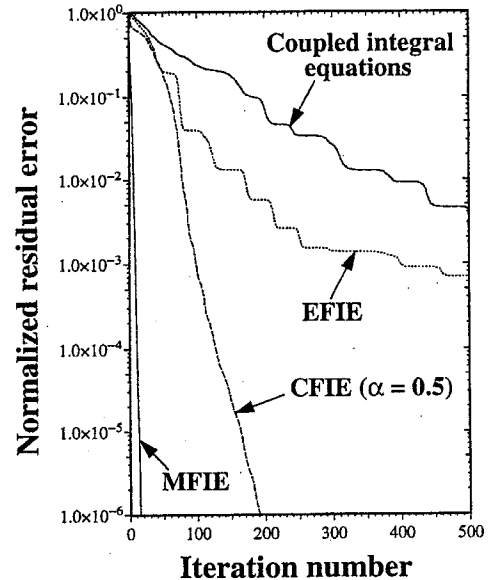

Fig. 6. Convergence speeds of the single integral equation formulations based on the MFIE, EFIE, and CFIE, respectively, compared with the convergence speed of the coupled integral equations formulation, for a dielectric sphere with $\varepsilon_2 = 4.0$ and $k_1 a = 0.5$.

computed equivalent electric and magnetic currents induced on the sphere for $\varepsilon_2 = 4.0$ are shown in Fig. 4. These results compare well with the exact results given by the series solution. Fig. 5 shows the corresponding computed radar cross section (RCS). Again, there is good agreement with the exact result.

Fig. 6 illustrates the convergence speeds of the single integral equation formulations based on the MFIE, EFIE, and CFIE, respectively, compared with that of the coupled integral equations formulation of [3], for a dielectric sphere with $\varepsilon_2 = 4.0, k_1 a = 0.5$ and $N = 912$. The convergence speeds of the three single integral equation formulations were greater than that of the coupled integral equations formulation. In particular, the single integral equation based on the MFIE converged almost two orders of magnitude faster than the coupled

integral equations. Unlike the case of a perfectly conducting object [11], however, the CFIE-based single integral equation containing 50% of EFIE ($\alpha = 0.5$) converged much slower than the MFIE-based single integral equation in the dielectric case.

As discussed in Appendix B, the singular integral equation based on the MFIE or EFIE is singular at the resonant frequencies of a cavity bounded by the surface S of the dielectric object, but filled with the material of the exterior region (μ_1, ε_1). The singularity of the MFIE-based single integral equation was investigated by choosing the parameter $k_1 a$ to correspond to the lowest internal resonance of the electric type, namely $k_1 a = 2.7439$. The number of edges
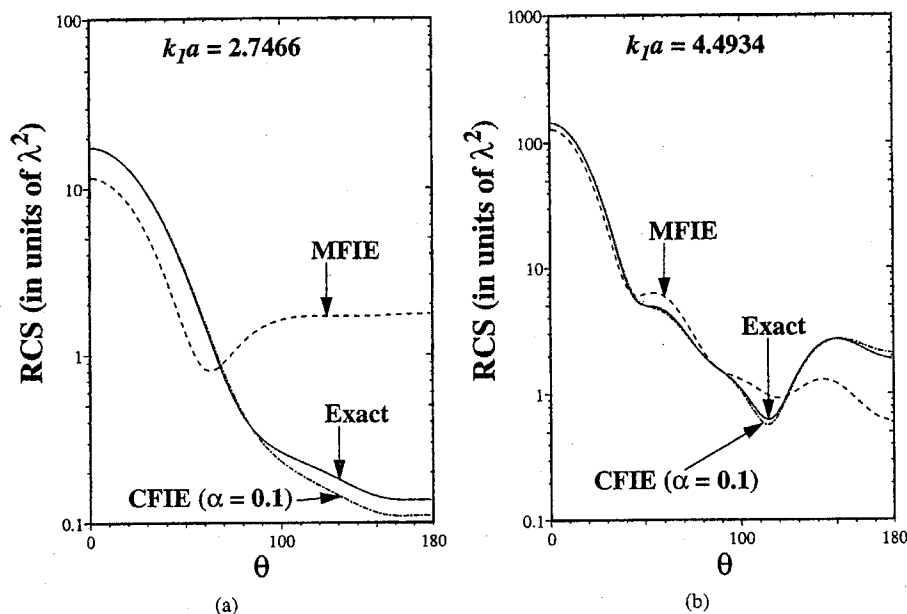
Fig. 7. Radar cross sections of dielectric spheres with $\varepsilon_2 = 2.25$ and radii corresponding to the lowest resonances of the (a) electric type and (b) magnetic type, respectively, for an empty cavity.

in the corresponding triangular-patch model was $N = 4560$ for $\varepsilon_2 = 2.25$. In this case, the MFIE-based single integral equation was found to converge, but to the wrong solution. Furthermore, the range of values of $k_1 a$ over which significant solution error was observed was found to be quite small, namely, within $\pm 1\%$ of the resonant value. The RCS results for $k_1 a = 2.7466$, where the solution error was found to be greatest, are shown in Fig. 7(a). To overcome this problem, the calculation was repeated for the CFIE-based single integral equation. A small value of $\alpha = 0.1$ was chosen to avoid significant reduction of the convergence speed as Fig. 6 would suggest. The corresponding RCS results are also shown in Fig. 7(a). It can be seen that CFIE-based single integral equation effectively eliminated the solution error at resonance.

The above calculations were repeated for the lowest internal resonance of the magnetic type, for which $k_1 a = 4.4934$. The number of edges in the corresponding triangular-patch model was $N = 9552$ for $\varepsilon_2 = 2.25$. The corresponding RCS results are shown in Fig. 7(b). It can be seen that the CFIE-based single integral equation again effectively eliminated the solution error produced by the MFIE-based single integral equation at resonance. It is of interest to note that a *small* value of $\alpha = 0.1$ in the CFIE actually resulted in a slight increase in the overall convergence speed at resonance compared with that of the MFIE. This can be seen in Fig. 8, which shows the convergence speeds of the MFIE- and CFIE-based single integral equations for the two resonances just discussed.

VI. CONCLUSION

In this paper, a single integral equation formulation for electromagnetic scattering by 3-D homogeneous dielectric objects is developed in which a single unknown effective current appears. Crucial to the formulation is the use of triangular-patch basis functions to expand the equivalent currents generated by the effective current. Numerical results for the scattering
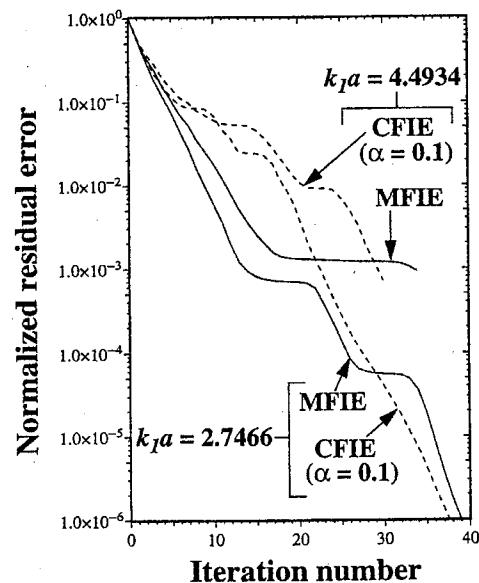

Fig. 8. Convergence speeds of the single integral equation formulations based on the MFIE and CFIE for the resonant dielectric spheres of Fig. 7. In the case of $k_1 a = 4.4934$, the iteration was stopped at a normalized residual error of 0.001 to save computation time.

of a plane wave by a dielectric sphere demonstrated the validity of the formulation. The convergence speed of the GMRES method for solving the matrix equation in the MFIE-based single integral equation formulation was found to be significantly greater than that of the coupled integral equations formulation. The CFIE-based single integral equation with $\alpha = 0.1$ was found to be effective in eliminating solution error at resonance. The formulation discussed in this paper can be generalized to the case of a homogeneous dielectric object embedded in a layered medium, by representing the interior fields in terms of a single effective current and employing the appropriate Green's functions for the layered exterior region.
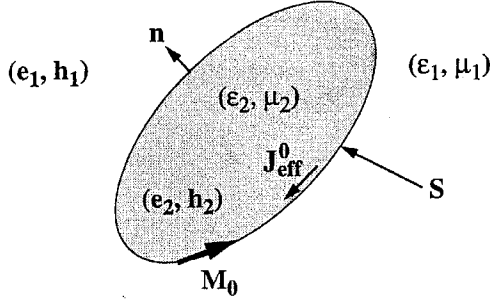
Fig. 9. Auxiliary problem for the single integral equation based on the MFIE at a resonant frequency of an empty cavity bounded by the surface S. $\mathbf{M}_0$ is the magnetic surface current density of the resonant mode, which acts as an external current source here.

APPENDIX A

The integral operators $\hat{\mathbf{E}}_1^s$ and $\hat{\mathbf{H}}_1^s$ for the exterior region are, for a time dependence of $e^{j\omega t}$, given by

$$\hat{\mathbf{E}}_1^s(\mathbf{J}, \mathbf{M}) = -j\omega\mathbf{A}_1 - \nabla\Phi_1 - \frac{1}{\varepsilon_1}\nabla \times \mathbf{F}_1 \quad (39)$$

$$\hat{\mathbf{H}}_1^s(\mathbf{J}, \mathbf{M}) = -j\omega\mathbf{F}_1 - \nabla\Psi_1 + \frac{1}{\mu_1}\nabla \times \mathbf{A}_1 \quad (40)$$

where

$$\mathbf{A}_1(\mathbf{r}) = \mu_1 \int_S \mathbf{J}(\mathbf{r}')G_1(\mathbf{r} - \mathbf{r}')\,dS' \quad (41)$$

$$\mathbf{F}_1(\mathbf{r}) = \varepsilon_1 \int_S \mathbf{M}(\mathbf{r}')G_1(\mathbf{r} - \mathbf{r}')\,dS' \quad (42)$$

$$\Phi_1(\mathbf{r}) = \frac{j}{\omega\varepsilon_1} \int_S \nabla' \cdot \mathbf{J}(\mathbf{r}')G_1(\mathbf{r} - \mathbf{r}')\,dS' \quad (43)$$

$$\Psi_1(\mathbf{r}) = \frac{j}{\omega\mu_1} \int_S \nabla' \cdot \mathbf{M}(\mathbf{r}')G_1(\mathbf{r} - \mathbf{r}')\,dS' \quad (44)$$

and $G_1(\mathbf{r} - \mathbf{r}')$ is given by (33). The integral operators $\hat{\mathbf{E}}_2^s$ and $\hat{\mathbf{H}}_2^s$ for the interior region are obtained from the above expressions by replacing the index 1 by 2 throughout.

APPENDIX B

In this Appendix, the MFIE, and EFIE for a dielectric object are shown to be singular at the resonant frequencies of a cavity bounded by the closed surface S of the object but filled with the material of the exterior region (μ_1, ε_1). First, consider the MFIE (16) and let the frequency coincide with a resonant frequency of the cavity. Then, there exists a magnetic current $\mathbf{M}_0$ on S which radiates a null field in the exterior region

$$\hat{\mathbf{E}}_1^s(0, \mathbf{M}_0)\big|_{\text{outside } S} = 0 \quad (45)$$

$$\hat{\mathbf{H}}_1^s(0, \mathbf{M}_0)\big|_{\text{outside } S} = 0. \quad (46)$$

Now, consider an auxiliary problem in which the magnetic current $\mathbf{M}_0$ acts as an external current source on the surface S of a cavity filled with the dielectric of parameters (μ_2, ε_2) and embedded in a medium of parameters (μ_1, ε_1), as illustrated in Fig. 9. This auxiliary problem obviously has a unique solution. Let the tangential fields in this solution just inside S be $\mathbf{n} \times \mathbf{e}_2$ and $\mathbf{n} \times \mathbf{h}_2$. The corresponding tangential fields $\mathbf{n} \times \mathbf{e}_1$

and $\mathbf{n} \times \mathbf{h}_1$ just outside S are determined by the boundary conditions

$$\mathbf{n} \times \mathbf{e}_1 = \mathbf{n} \times \mathbf{e}_2 - \mathbf{M}_0 \quad (47)$$

$$\mathbf{n} \times \mathbf{h}_1 = \mathbf{n} \times \mathbf{h}_2. \quad (48)$$

By the equivalence principle, the magnetic field $\mathbf{h}_1$ outside S can be written as

$$\begin{aligned} \mathbf{h}_1 &= \hat{\mathbf{H}}_1^s(\mathbf{n} \times \mathbf{h}_1, -\mathbf{n} \times \mathbf{e}_1)\big|_{\text{outside } S} \\ &= \hat{\mathbf{H}}_1^s(\mathbf{n} \times \mathbf{h}_1, -\mathbf{n} \times \mathbf{e}_2)\big|_{\text{outside } S} \end{aligned} \quad (49)$$

where (47) and (46) have been used. By the jump condition, when the integral operator on the RHS of (49) is evaluated inside S, the result is zero

$$\begin{aligned} 0 &= \hat{\mathbf{H}}_1^s(\mathbf{n} \times \mathbf{h}_1, -\mathbf{n} \times \mathbf{e}_2)\big|_{\text{inside } S} \\ &= \hat{\mathbf{H}}_1^s(\mathbf{n} \times \mathbf{h}_2, -\mathbf{n} \times \mathbf{e}_2)\big|_{\text{inside } S} \end{aligned} \quad (50)$$

where (48) has been used. It remains to show that the fields $\mathbf{e}_2$ and $\mathbf{h}_2$ in the interior region can always be represented in terms of a single effective electric current $\mathbf{J}_{\text{eff}}^0$; that is

$$\mathbf{n} \times \mathbf{e}_2 = \mathbf{n} \times \hat{\mathbf{E}}_2^s(\mathbf{J}_{\text{eff}}^0, 0)\big|_{\text{just inside } S} \quad (51)$$

$$\mathbf{n} \times \mathbf{h}_2 = \mathbf{n} \times \hat{\mathbf{H}}_2^s(\mathbf{J}_{\text{eff}}^0, 0)\big|_{\text{just inside } S}. \quad (52)$$

The integral operators on the RHS of the above equations are the familiar EFIE and MFIE integral operators for electromagnetic scattering by a perfectly conducting object embedded in a medium of parameters (μ_2, ε_2). It is well-known that the resonant frequencies of these operators in general do not coincide. Hence, at least one of (51) and (52) is nonsingular at any given frequency, which allows $\mathbf{J}_{\text{eff}}^0$ to be solved uniquely. Substituting (51) and (52) into (50), one obtains

$$0 = \hat{\mathbf{H}}_1^s\left[\mathbf{n} \times \hat{\mathbf{H}}_2^s(\mathbf{J}_{\text{eff}}^0, 0), -\mathbf{n} \times \hat{\mathbf{E}}_2^s(\mathbf{J}_{\text{eff}}^0, 0)\right]\big|_{\text{inside } S}. \quad (53)$$

Equation (53) shows that the solution $\mathbf{J}_{\text{eff}}^0$ to the auxiliary problem of Fig. 9 is a nontrivial solution in the null space of the integral operator on the RHS of (16). This means that the MFIE (16) is singular at the resonant frequency under consideration.

By duality, the EFIE (15) is singular at the same frequency. In this case, however, the corresponding solution $\mathbf{J}_{\text{eff}}^1$ in the null space of the integral operator on the RHS of (15) is the solution of a different auxiliary problem, where the magnetic current $\mathbf{M}_0$ shown in Fig. 9 is replaced by an *electric* current $\mathbf{J}_1 = \sqrt{\epsilon_0/\mu_0}\mathbf{M}_0$ radiating a null field in the exterior region. Obviously, $\mathbf{J}_{\text{eff}}^1$ is different from $\mathbf{J}_{\text{eff}}^0$. This suggests that, although the MFIE (16) and EFIE (15) are individually singular at the same resonant frequency, a linear combination of the MFIE and EFIE, namely CFIE $= [(1-\alpha)\Delta]$ MFIE $+ \alpha\sqrt{\epsilon_0/\mu_0}$ EFIE, where $0 < \alpha < 1.0$ and Δ is the average side length of the triangular-patch model, is nonsingular at all frequencies, since the null spaces of the integral operators in (15) and (16) are disjoint.

REFERENCES

[1] A. J. Poggio and E. K. Miller, "Integral equation solutions of three-dimensional scattering problems," in *Computer Techniques for Electromagnetics*, R. Mittra, Ed.   New York: Pergamon, 1973.

[2] J. R. Mautz and R. F. Harrington, "H-field, E-field and combined-field solutions for conducting bodies of revolution," *Archiv Elecktronik Uebertragungstechnik (AEU)*, Germany, vol. 32, pp. 157–164, 1978.

[3] K. Umashankar, A. Taflove, and S. M. Rao, "Electromagnetic scattering by arbitrary shaped three-dimensional homogeneous lossy dielectric objects," *IEEE Trans. Antennas Propagat.*, vol. AP-34, pp. 758–766, June 1986.

[4] D. Maystre, "Integral methods," in *Electromagnetic Theory of Gratings*, R. Petit, Ed.   New York: Springer-Verlag, 1980.

[5] E. Marx, "Single integral equation for wave scattering," *J. Math. Phys.*, vol. 23, pp. 1057–1065, 1982.

[6] E. Marx, "Integral equation for scattering by a dielectric," *IEEE Trans. Antennas Propagat.*, vol. AP-32, pp. 166–172, Feb. 1984.

[7] A. W. Glisson, "An integral equation for electromagnetic scattering from homogeneous dielectric bodies," *IEEE Trans. Antennas Propagat.*, vol. AP-32, pp. 173–175, Feb. 1984.

[8] S. M. Rao, D. R. Wilton, and A. W. Glisson, "Electromagnetic scattering by surfaces of arbitrary shape," *IEEE Trans. Antennas Propagat.*, vol. AP-30, pp. 409–418, May 1982.

[9] S. M. Rao and D. R. Wilton, "E-field, H-field and combined field solution for arbitrarily shaped three-dimensional dielectric bodies," *Electromagn.*, vol. 10, pp. 407–421, 1990.

[10] Y. Saad and M. H. Schultz, "GMRES: A generalized minimal residual algorithm for solving nonsymmetric linear systems," *SIAM J. Sci. Stat. Comput.*, vol. 7, pp. 856–869, 1986.

[11] D. R. Wilton and J. E. Wheeler, "Comparison of convergence rates of the conjugate gradient method applied to various integral equation formulations," in *Application of Conjugate-Gradient Methods in Electromagnetics and Signal Analysis*, T. K. Sarkar, Ed.   Amsterdam, The Netherlands: Elsevier, 1991.

Michael S. Yeung received the B.S. degree in physics from California Institute of Technology, Pasadena, and the Ph.D. degree in electrical engineering from the University of California at Berkeley, in 1972 and 1995, respectively.

From 1982 to 1989, he was with Intel, Santa Clara, CA, where he worked on photolithography process development and simulation. From 1990 to 1995 he was a Graduate Student Researcher in the Department of Electrical Engineering and Computer Sciences, University of California at Berkeley, where he worked on quantum optics and the fast multipole method for electromagnetic scattering. Since 1995 he has been with Boston University, Boston, MA, where he is now an Assistant Professor in the Department of Manufacturing Engineering. His current research interests include the application of the method of moments and the finite-difference time-domain and finite-element time-domain algorithms to the simulation of electromagnetic scattering phenomena in microchip manufacturing.